9114 *J. Phys. Chem. A* **2002,** *106,* 9114−9119

Halogen Bond in $(CH_3)_nX$ (X = N, P, *n* = 3; X = S, *n* = 2) and $(CH_3)_nXO$ (X = N, P, *n* = 3; X = S, *n* = 2) Adducts with CF_3I. Structural and Energy Analysis Including Relativistic Zero-Order Regular Approximation Approach in a Density Functional Theory Framework

Pina Romaniello and Francesco Lelj*

LaMI Dipartimento di Chimica and LaSCAMM, INSTM Sezione Basilicata, Università della Basilicata, Via N. Sauro 85, 85100 Potenza, Italy

Received: January 18, 2002; In Final Form: June 24, 2002

Density functional theory (DFT) calculations on the geometry and bonding energy of the X- - -I *inter*molecular interaction of CF_3I and $(CH_3)_nX$ (X = N, P, *n* = 3; X = S, *n* = 2) and $(CH_3)_nXO$ (X = N, P, *n* = 3; X = S, *n* = 2) are reported. The effect of the basis set, Effective Core Potential (ECP), and relativistic corrections have been investigated to gain insight into the origin and nature of this interaction. Energy decomposition in terms of different contributions allows us to understand the different donor behavior of second and third row atoms toward perfluorinated iodo hydrocarbon compounds, suggesting that bond energies are mainly due to orbital contribution. TD-DFT calculations of the van der Waals coefficient C_6 for CF_3I- - -$N(CH_3)_3$ and CF_3I- - -$P(CH_3)_3$ adducts estimate values of −2.02 and −1.30 kcal/mol, respectively, for their dispersion energy, thus representing only a small contribution to the total bonding energy (−5.64 and −5.76 kcal/mol, respectively). The role of competition between *intra*- and *inter*molecular donation has been elucidated. All the adducts with oxides as donors show a weaker interaction with CF_3I than the relative donor without oxygen except the CF_3I- - -$ON(CH_3)$ adduct, which has a stronger interaction. Basis set superposition errors (BSSE) are very relevant in describing the relative order of stability of the oxide of trimethyl derivatives of group 15 elements . Explicit scalar relativistic (s.r.) ZORA (zero-order regular approximation) corrections are essential to reproduce correctly geometrical parameters and bonding energies involving X- - -I interaction.

1. Introduction

The relevance of *inter*molecular interactions of substantial stability stems from their possible applications in different fields such as in new materials engineering[1,2] and chemical and biological process studies.[3,4]

The technological importance of perfluorocarbon (PCF) compounds has focused the interest on intermolecular interactions between carbon-bound halogen atoms (X) and electronegative atoms (El).[5−8]

An accurate study on C−X- - -El (X = F, Cl, Br, I and El = N, O, S) interaction led by Lommerse et al.[9] has demonstrated that if the carbon-bound halogen atom is in a sufficiently electron-withdrawing environment, then a strong attractive overall interaction will exist. Besides, a recent study[7] on interaction involving ammonia and halofluoromethanes has shown that the bonding energies of CF_3X- - -NH_3 increase from 2 to 6 kcal/mol moving along the series X = Cl, Br, I, and the progressive introduction of F atoms in methyliodides raises the interaction energy from 3 kcal/mol for CH_3I to 6 kcal/mol for CF_3I. This is a very important result, because halogen bonding involving perfluorinated alkyl halides and appropriate donors can be comparable in strength to hydrogen bonding (typical H-bonded interaction energies vary between 2 and 15 kcal/mol).[10] These results offer new opportunities in the manipulation of molecular aggregation, which is useful in many fields. For these reasons the intermolecular interaction between CF_3I and different donors D (D = $(CH_3)_3N$, $(CH_3)_3P$, $(CH_3)_2S$, $(CH_3)_3NO$, $(CH_3)_3PO$, and DMSO) has been analyzed to evaluate the role of the donor on the adduct geometry and on the strength of the interaction.

2. Method

The DFT calculations on the geometry and bonding energy of the X- - -I intermolecular interaction of CF_3I and $(CH_3)_nX$ (X = N, P, *n* = 3; X = S, *n* = 2), $(CH_3)_nXO$ (X = N, P, *n* = 3; X = S, *n* = 2) have been performed with the ADF2000 package.[11] This program allows us to consider relativistic effects[12] by means of the ZORA[13] (zero order regular approximation) approach. This variationally stable scheme is based on a regular-potential expansion and produces a Hamiltonian that in zeroth order reproduces all important relativistic effects including the spin−orbit interaction:

$$H^{\mathrm{ZORA}} = V + \vec{\sigma}\cdot\vec{\mathrm{p}}\,\frac{c^2}{2c^2 - V}\vec{\sigma}\cdot\vec{\mathrm{p}}$$

(for a particle that is moving in a potential *V*).

A valence double-ζ STO basis set with one polarization function for main element atoms and a triple-ζ 3d,4s basis set with one 4p function for I and frozen cores (C, N, O, F: 1s; S, P: 1s−2p; I: 1s−4d) have been used for nonrelativistic calculations, and an optimized valence basis set that is of the same size as the nonrelativistic basis set described above, for relativistic calculations.[14] The Becke functional for the exchange[15] (B) and the Perdew functional for the correlation[16] (P) have been used.

Further calculations have been carried out for comparative purposes with the Gaussian98[17] A.7 program. To evaluate the performance of different combinations of Gaussian basis set and/or ECP, a preliminary study of the CF_3I- - -$N(CH_3)_3$ adduct geometry has been performed using different basis sets: 3-21g* (I);[18] Ahlrichs TVZ on all atoms and LanLDZdp ECP on the I

---

* Corresponding author. E-mail: lelj@unibas.it.

10.1021/jp0255334 CCC: $22.00

TABLE 1: I- -N Bond Distance Calculated at the B3LYP Level with the Following Basis Sets: 3-21g* (I), Ahlrichs on All Atoms and LanLDZdp ECP on the I Atom (II), Ahlrichs on All Atoms and Stuttgart RLC ECP on the I Atom (III), 6-31g* on All Atoms and 6-311g* on the I Atom (IV)

basis set	CF_3I- - -$N(CH_3)_3$ distance (Å)
I	2.709
II	2.714
III	2.720
IV	2.931
exp[a]	2.84 ± 0.03

[a] Reference 7.

atom (II);[19,20] Ahlrich TVZ on all atoms and Stuttgart RLC ECP on the I atom (III);[21] 6-31g* on all atoms and 6-311g* on the I atom (IV).[22,23] As shown in Table 1, the last one gives the best results as far as the I- - -N bond length is concerned, where relativistic corrections are not explicitly included.

The energy minima of all these structures have been confirmed by frequency calculations at the 3-21g*/B3LYP[24] level.

The interaction between the CF_3I and the donor has been analyzed by using the fragment analysis proposed by Ziegler and Rauk.[25−27] The interaction energy (ΔE_{int}) is split into two physically meaningful terms:

$$\Delta E_{\text{int}} = \Delta E° + \Delta E_{\text{oi}}$$

$\Delta E°$ is known as the steric repulsion energy and consists of two components: the classical electrostatic interaction (ΔE_{elstat}) between the unperturbed charge distributions of the interacting fragments, usually attractive, and the so-called Pauli repulsion (ΔE_{Pauli}), due essentially to the Pauli principle. The steric term is usually repulsive at the equilibrium distance because the repulsive component ΔE_{Pauli} dominates, such as in this work.

The ΔE_{oi} term takes the attractive orbital interactions into account and can be split into the additive contributions from the various irreducible representations Γ of the overall point group symmetry of the system. In the case of closed-shell fragments, such as in the present work, the orbital interaction term ΔE_{oi} accounts for the charge transfer (interaction between occupied and virtual orbitals of separate fragments) and polarization (empty/occupied orbital mixing on one fragment). In the case of open-shell fragments, ΔE_{oi} contains also the energy gained due to the formation of the electron pair bonds.

TD-DFT calculations, involving the asymptotically correct Van Leeuwen−Baerends potential (LB94),[28] have been performed to estimate the dispersion energy, governed by the isotropic van der Waals dispersion coefficient C_6:

$$E_{\text{disp}}(\text{A,B}) = -\frac{C_6(\text{A,B})}{{R_{\text{AB}}}^6}$$

where R_{AB} is the distance between the A and B centers of mass. The dispersion coefficient C_6 can be calculated from the polarizabilities of the two monomers at imaginary frequencies iω.[29]

3. Results and Discussion

The geometries of adducts have been fully optimized at the DFT level. All adducts have a C_s symmetry, except those with $(CH_3)_3N$ and $(CH_3)_3P$, which belong to the C_{3v} point group, and with $(CH_3)_3PO$ and DMSO (interacting by S atom), which belong to the C_1 point group.

TABLE 2: Bond Distances (Å) and Angles (deg) for Adducts 1 (symmetry C_{3v}), 2 (symmetry C_{3v}), and 3 (symmetry C_s) Calculated with Nonrelativistic DFT at the B3LYP/Basis Set IV Level (n.r. B3LYP) and at the BP Level (n.r. BP) and with Scalar Relativistic ZORA DFT at the BP Level (s.r. ZORA)

	method	**1**	**2**	**3**
I- - -X distance (X = N, P, S) (Å)	n.r. B3LYP	2.931	3.396	3.427
	n.r. BP	2.933	3.302	3.352
	s.r. ZORA	2.883	3.195	3.259
I−C distance (Å)	n.r. B3LYP	2.203	2.206	2.199
	n.r. BP	2.273	2.285	2.275
	s.r. ZORA	2.268	2.287	2.271
C−F[a] distance (Å)	n.r. B3LYP	1.340	1.340	1.338
	n.r. BP	1.353	1.354	1.353
	s.r. ZORA	1.354	1.355	1.353
C−I- - -X angle (deg)	n.r. B3LYP	180.00	180.00	97.77
	n.r. BP	180.00	180.00	98.87
	s.r. ZORA	180.00	180.00	96.11

[a] The average value of three C−F distances has been reported in the case of the adduct **3**.

TABLE 3: Mulliken Gross Population of Kohn−Sham SCF Orbitals of CF_3I and Donor D (D = $(CH_3)_3N$, $(CH_3)_3P$, $(CH_3)_2S$) Fragments in 1−3 Calculated at the s.r. ZORA Level

Γ			**1** $(^1A_1)^a$	**2** $(^1A_1)^a$	Γ			**3** $(^1A')^a$
A_1	CF_3I	$5a_1$	1.99	1.98	A′	CF_3I	10a′	1.99
		$6a_1$(LUMO)	0.12	0.17			11a′ (LUMO)	0.12
	D	$4a_1$ (HOMO)	1.88	1.87		D	6a′ (HOMO)	1.90
A_2	CF_3I	$1a_2$ (HOMO)	2.00	2.00	A″	CF_3I	6a″ (HOMO)	1.99
	D	$1a_2$ (HOMO)	2.00	2.00		D	4a″ (HOMO)	2.00
E_1	CF_3I	$5e_1$ (HOMO)	1.99	1.98				
	D	$4e_1$ (HOMO)	2.00	2.00				

[a] The ground state configuration has been reported in parentheses.

TABLE 4: Contributions to the Bonding Energy (kcal/mol) for Adducts 1−3 in Terms of CF_3I and $(CH_3)_3N$, $(CH_3)_3P$, and $(CH_3)_2S$ Neutral Fragments Calculated at the s.r. ZORA Level

contributions to the I- - -X (X = N, P) bonding energy (kcal/mol)	**1**	**2**	contributions to the I- - -S bonding energy (kcal/mol)	**3**
ΔE_{Pauli} (eV)	18.83	25.27	ΔE_{Pauli} (eV)	15.11
ΔE_{elstat}	−15.59	−18.63	ΔE_{elstat}	−11.36
ΔE^0	3.24	6.64	ΔE^0	3.75
ΔE^{A1}	−9.81	−11.82	$\Delta E^{\text{A}'}$	−8.27
ΔE^{A2}	−0.01	0.00	$\Delta E^{\text{A}''}$	−0.48
ΔE^{E}	−1.08	−1.37		
ΔE_{oi}	−10.89	−13.19	ΔE_{oi}	−8.75
$\Delta E_{\text{oi}} + \Delta E^0$	−7.65	−6.55	$\Delta E_{\text{oi}} + \Delta E^0$	−5.00
BSSE CF_3I + $(CH_3)_3X$(ghost)	−0.71	−0.53	BSSE CF_3I + $(CH_3)_2S$(ghost)	−0.53
BSSE $(CH_3)_3X$ + CF_3I(ghost)	−1.30	−0.26	BSSE $(CH_3)_2S$ + CF_3I(ghost)	−0.60
$\Delta E_{\text{oi}} + \Delta E^0$ (corrected for BSSE)	−5.64	−5.76	$\Delta E_{\text{oi}} + \Delta E^0$ (corrected for BSSE)	−3.87

Tables 2 and 4 report some selected equilibrium bond distances and angles and the interaction energies, respectively, for the adducts with $(CH_3)_3N$ (**1**), $(CH_3)_3P$ (**2**), and $(CH_3)_2S$ (**3**) as donors.

The relevance of the relativistic effects on the I- - -N distance is evident in the case of the adduct **1** if compared to the experimental distance found in cocrystals of α,ω-diiodoperfluoroalkanes with different diamines (2.84 ± 0.03 Å):[5−7] the I- - -N bond contraction observed at the scalar relativistic (s.r.) ZORA level accurately describes this distance. This result

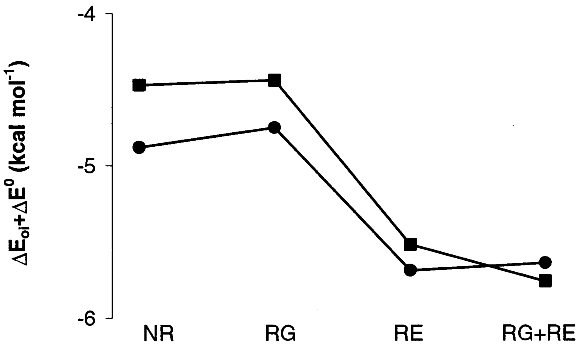

Figure 1. BSSE-corrected bonding energy (kcal mol^{-1}) for adducts **1** (●) and **2** (■) in terms of CF_3I, $(CH_3)_3N$, and $(CH_3)_3P$ neutral fragments, respectively, calculated at nonrelativistic (NR), relativistic bonding energy (RE), relativistic geometry (RG) and RG+RE level.

suggests that also other I- - -X distances are described very well at the (s.r.) ZORA level.

Other distances are only marginally affected by relativistic effects. In particular, as the calculated values at the BP level suggest (Table 2), the C−I bond undergoes a negligible contraction (0.005 Å) if compared to that of the I- - -N bond (0.05 Å).

The formation of the adducts yields an elongation of the I−C bond (2.230 Å in the CF_3I monomer), more pronounced in adduct **2**. The C−F bonds are also elongated by about 0.01 Å upon formation of the adduct (1.345 Å in the CF_3I monomer). These bond elongation effects can be explained by a small charge transfer from the donor HOMO to the CF_3I LUMO (Table 3): in the last one there are antibonding interactions between I−C orbitals and between C−F orbitals.

We have calculated the interaction energies for the adducts formation using the decomposition scheme reported in the Method section.

A preliminary study on the interactions I- - -N and I- - -P has highlighted the importance of relativistic effects at both geometry and energy bonding level. In fact, our calculations reproduce the literature trend N < P only if the relativistic geometry and energy bonding are used, as Figure 1 shows. Thus, the relativistic corrections have been considered not only in the geometry optimization procedures but also in the bonding energy calculations.

However, the generalized gradient-approximated (GGA) energy functionals used in density functional theory (DFT) do not describe the small van der Waals interaction energies.[30] Despite this, the time-dependent density functional theory can be used to obtain the van der Waals dispersion coefficients that determine the long-range dispersion part of a potential energy surface of two interacting (distant) molecules. Thus, the C_6 van der Waals coefficient has been calculated for adducts **1** and **2** and their dispersion energy has been estimated to be −2.02 and −1.30 kcal mol^{-1}, respectively, without any significant effect of basis set increase. These findings suggest that the contribution of dispersion energy for all the studied adducts is small, owing to the strong polarization of the I- -(CF_3) bond. As a qualitative measure of this effect, it might be pointed out that the difference of Mulliken charges of I and C in CF_3I and CH_3I are respectively 0.90 and 0.18. Hence, the Ziegler and Rauk analysis can be considered a valid tool for describing the interaction of these adducts.

On the basis of the results reported in Table 4, the orbital interaction term ΔE_{oi} seems to be important in the I- - -X interaction, because the order in which the interaction becomes stronger (S < N < P) corresponds to the increase in this contribution. It is noteworthy that the trend of the interaction energies described above refers to the values corrected for BSSE.[31] Without this correction the I- - -N interaction is stronger than the I- - -P one. Besides, the calculated value for the adduct **1** is in good agreement with the experimental one of 5.0 ± 0.1 kcal/mol for the association of CF_3I with 2,4,6-trimethylpyridine in cyclopentane solution by temperature-dependent NMR spectroscopy and of 7.4 kcal/mol for the 1-iodoperfluorohexane and liquid 2,2,6,6-tretramethylpiperidine measured with an adiabatic accelerating rate calorimeter.[7]

As regards the individual contribution to the orbital interaction term, the ΔE^{A1} term ($\Delta E^{A'}$ in the adduct **3**), which accounts for the σ-donation from the donor HOMO to the CF_3I LUMO, is the largest one. The larger charge transfer in the adduct **2** is evidently ascribed to a better interaction between the $(CH_3)_3P$ MOs and the CF_3I MOs. In particular, the larger charge transfer from the $(CH_3)_3P$ HOMO to the CF_3I LUMO can be attributed to a better interaction between the $(CH_3)_3P$ $4a_1$ orbital and the CF_3I $6a_1$ orbital, as the composition of these MOs in terms of CF_3I and the donor neutral fragment orbitals suggests (Figure 2).

Indeed, these two MOs have a bonding interaction in the adduct $9a_1$ (HOMO) orbital, whereas the adduct $10a_1$ (LUMO) one is the antibonding counterpart. The donor $4a_1$ orbital (**6a′**

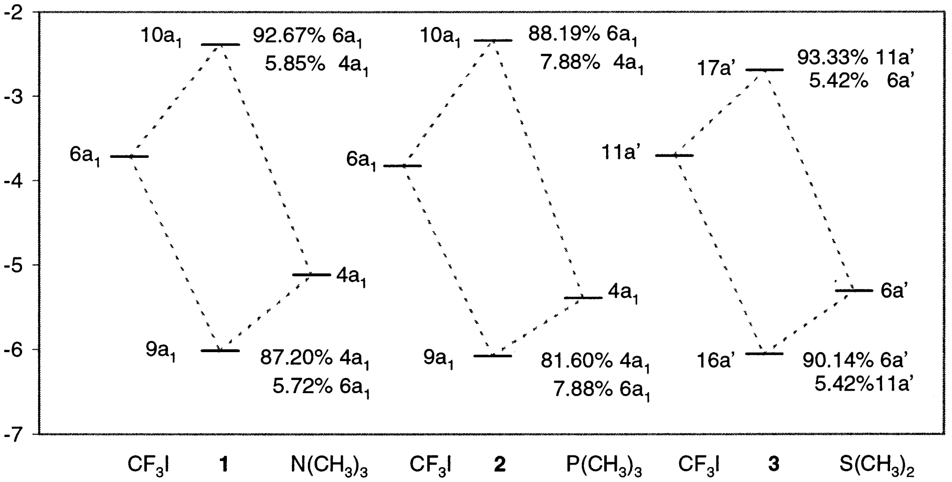

Figure 2. HOMOs and LUMOs energy diagram for the CF_3I- - -$N(CH_3)_3$ (**1**), CF_3I- - -$P(CH_3)_3$ (**2**), and CF_3I- - -$S(CH_3)_2$ (**3**) adducts (**1** and **2** belonging to the C_{2v} point group and **3** to the C_s one) calculated at scalar relativistic (s.r.) ZORA level in terms of two neutral fragments CF_3I and donor D (=$(CH_3)_3N$, $(CH_3)_3P$, $(CH_3)_2S$).

TABLE 5: Bond Distances (Å) and Angles (deg) for Adducts CF_3I- -$ON(CH_3)_3$ (4) (Symmetry C_s), CF_3I- -$OP(CH_3)_3$ (5) (Symmetry C_1), 6′ (Symmetry C_1), 6″ (Symmetry C_s), and 6‴ (Symmetry C_s) Calculated with Nonrelativistic DFT at the B3LYP/Basis Set IV Level (n.r. B3LYP) and at the BP Level (n.r. BP) and with Scalar Relativistic ZORA DFT at BP Level (s.r. ZORA)

method		**4**	**5**	**6″**	**6‴**		**6′**
n.r. B3LYP	I- - -O distance (Å)	2.715	2.856	2.847	2.876	I- - -S distance (Å)	3.584
n.r. BP		2.821	2.998	2.964	3.032		3.587
s.r. ZORA		2.768	2.923	2.908	2.967		3.470
n.r. B3LYP	I−C distance (Å)	2.203	2.184	2.191	2.187	I−C distance (Å)	2.198
n.r. BP		2.273	2.239	2.248	2.240		2.255
s.r. ZORA		2.269	2.236	2.244	2.235		2.253
n.r. B3LYP	C−F[a]distance (Å)	1.344	1.341	1.340	1.340	C−F[a] distance (Å)	1.334
n.r. BP		1.356	1.353	1.351	1.352		1.347
s.r. ZORA		1.357	1.353	1.352	1.352		1.347
n.r. B3LYP	I- - -O−X angle (X = N, P, S) (deg)	121.34	139.40	130.45	122.31	I- - -S−O angle (deg)	141.32
n.r. BP		118.79	127.97	124.14	112.49		130.29
s.r. ZORA		117.79	121.47	122.09	110.58		131.46

[a] The average value of three C−F distances has been reported.

TABLE 6: Contributions of the Bonding Energy (kcal/mol) for Adducts 4, 5, 6′, 6″, and 6‴ in Terms of CF_3I and $(CH_3)_3NO$, $(CH_3)_3PO$, and $(CH_3)_2SO$ Neutral Fragments Calculated at the s.r. ZORA Level

contributions to the I- - -O bonding energy (kcal/mol)	**4**	**6″**	**6‴**	contributions to the I- - -X (X = O, S) bonding energy (kcal/mol)	**5**	**6′**
ΔE_{Pauli}	20.27	11.55	8.44	ΔE_{Pauli}	9.73	6.47
ΔE_{elstat}	−16.58	−9.43	−7.93	ΔE_{elstat}	−9.12	−3.43
ΔE^0	3.68	2.12	0.52	ΔE^0	0.61	3.03
$\Delta E^{A'}$	−12.38	−6.40	−4.22	ΔE^{A}	−5.51	−5.11
$\Delta E^{A''}$	−0.65	−0.40	−0.19			
ΔE_{oi}	−13.03	−6.80	−4.41	ΔE_{oi}	−5.51	−5.11
$\Delta E_{oi} + \Delta E^0$	−9.35	−4.67	−3.89	$\Delta E_{oi} + \Delta E^0$	−4.90	−2.08
BSSE $CF_3I + (CH_3)_nYO$(ghost)	−0.49	−0.42	−0.32	BSSE $CF_3I + (CH_3)_nYO$(ghost)	−0.46	−0.45
BSSE $(CH_3)_nYO + CF_3I$(ghost) (Y = N, S)	−1.05	−0.93	−0.37	BSSE $(CH_3)_nYO + CF_3I$(ghost) (Y = P, S)	−0.50	−0.69
$\Delta E_{oi} + \Delta E^0$ (corrected for BSSE)	−7.81	−3.32	−3.20	$\Delta E_{oi} + \Delta E^0$ (corrected for BSSE)	−3.94	−0.94

in the adduct **3**) is a X *n*p (X = N, P, S) based orbital, and it is destabilized by an antibonding interaction with hydrogen 1s orbitals, more strongly in the $(CH_3)_3N$ donor, so that there is a better energy match between the CF_3I $6a_1$ and donor $4a_1$ orbitals in the adduct **1**. On the other hand, the overlap $6a_1/4a_1$ is larger in adduct **2** because the P $3p_z$ orbital is more diffuse, in fact, the SFO (symmetry-adapted combination of fragment MOs) overlap matrix $6a_1/4a_1$ (**11a′**/**6a′** in the adduct **3**) is 0.129, 0.210, and 0.140 for N, P, and S, respectively). The interplay of these two factors yields a better interaction in the case of the adduct **2**.

As regards the adducts with the oxides, we have found a I- - -O distance that is shorter than the relative donor without oxygen, as also experimentally found in pyridine derivatives and corresponding *N*-oxides (the N- - -I−C and O- - -I−C distances are 2.864(2) and 2.754(2) Å, respectively).[32]

It is noteworthy that in the interaction with the DMSO, the I atom can interact with either the S atom (**6′**) or the O atom in two different regiochemistries that we have denoted with **6″** and **6‴** (Figure 3). The I- - -S distance is longer than that in the adduct **3** (Table 5).

Whereas the first row atom based donor shows a weaker interaction with the CF_3I than the relative oxide, in agreement with experimental evidence,[32] the second row atom based donors show a stronger interaction. On the basis of our calculations the orbital interaction term is responsible for this bonding energy trend. To get a deeper insight into the influence of the O−X (X = N, P, S) intramolecular interaction on the CF_3I- - -D (D = $(CH_3)_3N$, $(CH_3)_3P$, $(CH_3)_2S$, $(CH_3)_3NO$, $(CH_3)_3PO$, and DMSO) intermolecular interaction a study of the electronic structure of the donors has been undertaken.

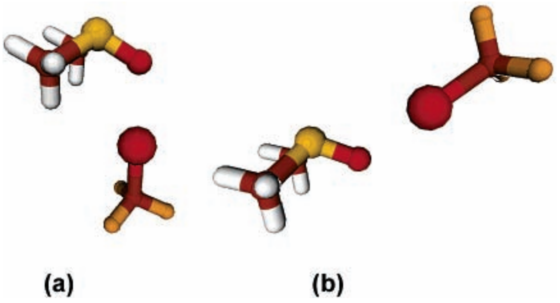

Figure 3. Two possible geometries for the interaction between CF_3I and the oxygen atom in the case of DMSO as donor [adducts **6″** (a) and **6‴** (b)].

TABLE 7: Percentage Composition (%) of the HOMO Donor in Terms of Single Atom Fragments

donor	O	X = N, P, S	C	H
$(CH_3)_3N$		66.42 ($2p_z$)	5.58	27.81 (1s)
$(CH_3)_3P$		74.03 ($3p_z/3s$)	12.41 ($2p_x/2p_z$)	13.15 (1s)
$(CH_3)_2S$		86.96 ($2p_y$)	2.06	10.06 (1s)
$(CH_3)_3NO$	88.11 ($2p_x/2p_y$)	1.48	4.86	4.66
$(CH_3)_3$ PO	73.43 ($2p_x/2p_y$)	12.33 ($3d_{x^2-y^2}$)	9.51	3.13
DMSO (**6′**)	59.08 ($2p_x/2p_z$)	26.06 ($3p_x$)	8.89	6.35
DMSO (**6″**)	61.48 ($2p_x/2p_y$)	24.57 ($3p_x$)	8.67	6.21
DMSO (**6‴**)	62.33 ($2p_y$)	23.40 ($3p_y$)	8.87	6.00

The donor HOMO, mainly involved in the interaction with CF_3I, is essentially localized on the X *n*p orbitals (X = N, P, S) in the interactions involving $(CH_3)_3N$, $(CH_3)_3P$, and $(CH_3)_2S$ as donors, and on the O *n*p orbitals in those involving the oxides (Table 7). The analysis in terms of the neutral fragments X (=$(CH_3)_3N$, $(CH_3)_3P$, $(CH_3)_2S$) and O shows the influence of charge transfer between the O 2p orbitals and the X (=N, P, S) *n*p orbitals on the CF_3I- - -donor interaction.

TABLE 8: CHELPG and Mulliken Charges (e) for Isolated Donors Involving in 1−6‴ Adducts

	O		X^a		C	
adduct	CHEPG	Mulliken	CHEPG	Mulliken	CHEPG	Mulliken
1			−0.221	−0.607	−0.269	0.126
2			−0.197	−0.020	−0.273	−0.164
3			−0.154	0.050	−0.420	−0.294
4	−0.582	−0.684	0.400	−0.210	−0.459	0.120
5	−0.645	−0.734	0.909	0.742	−0.562	−0.191
6′	−0.417	−0.753	0.289	0.834	−0.442	−0.328
6″	−0.415	−0.752	0.283	0.828	−0.452	−0.327
6‴	−0.423	−0.754	0.298	0.827	−0.467	−0.325

[a] X = N, P, S.

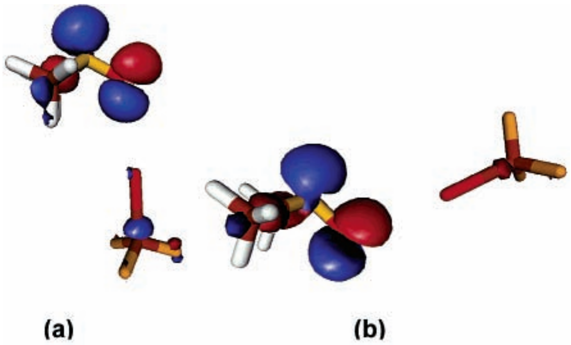

Figure 4. Sketches of HOMOs for **6″** (a) and **6‴** (b).

In the $(CH_3)_3NO$ donor there is a charge transfer from $(CH_3)_3N$−HOMO, mainly localized on the N atom, to the empty O $2p_y$ orbital (which acquires a charge of 1.04 e), which receives electrons from the O p_x orbital (whose population decreases to 1.77 e) as well. There is also a small charge transfer from the O $2p_z$ orbital (whose population decreases to 1.85 e) to the $(CH_3)_3N$ virtual orbitals. Also in the $(CH_3)_3PO$ donor a "charge exchange" is observed, but it seems more relevant. In fact, the empty O $2p_y$ orbital receives a charge of 1.46 e from the $(CH_3)_3P$ HOMO (13a′), mainly localized on the P atom, whereas the O $2p_x/p_z$ orbitals (whose populations decrease to 1.59 and 1.66 e, respectively) transfer charge to $(CH_3)_3P$ virtual orbitals, in particular to the $(CH_3)_3P$ 15a′ (0.20 e) and $(CH_3)_3P$ 16a′ (0.20 e) ones.

In the $(CH_3)_2SO$ donor there is a strong charge transfer between O and $(CH_3)_2S$, as well. The O atom receives electrons in its empty *n*p orbitals ($2p_z = 1.51$ e, $2p_y = 1.36$ e, $2p_x = 1.28$ e, for **6′**, **6″**, and **6‴**, respectively) and transfers electrons from full *n*p orbitals (depleting their populations as follows: $2p_x = 1.59$ e and $2p_y = 1.63$ e, $2p_x = 1.67$ e and $2p_z = 1.70$, $2p_y = 1.76$ e and $2p_z = 1.70$, for **6′**, **6″**, and **6‴**, respectively).

On the basis of these results, the larger stability of adduct **4** in comparison to adducts **1** and **5**, and of adduct **2** in comparison to adduct **5**, can be explained: the O atom is enough electron-rich to be a better donor than the N atom in adduct **1**. In adduct **5**, instead, the O atom prefers to release electrons to the P atom instead of the I atom. On the other hand, the calculated CHELPG and Mulliken charges of the isolated donors (Table 8) show that the O atom in $(CH_3)_3NO$ has a larger tendency to delocalize its charge on the I atom than in $(CH_3)_3PO$ because it is near the N atom, which has a less positive charge than the P atom.

Similarly, one can understand the smaller stability of the adducts **6′**, **6″**, and **6‴** in comparison with the adducts **3**−**5**.

It is interesting to explain the interaction energy trend in the adducts with DMSO. The interaction of the I atom on the O atom of the DMSO is more preferred than that on the S atom. As reported in Table 6, the steric term ΔE^0 makes the interaction I- - -S weaker than the I- - -O one. Indeed, the adduct **6′** shows a weaker electrostatic contribution due to the strongly positive charged S atom close to the positively charged I atom.

Besides, it is worth noting the substantial difference in the orbital interaction term between adduct **6″** and **6‴**, essentially due to the different overlap contribution to the interaction between CF_3I and DMSO orbitals. In particular, in Figure 4 sketches of HOMOs for **6″** and **6‴** are reported; (SFO overlap matrix DMSO-HOMO/CF3I-LUMO, which are mainly involved in the charge transfer (Table 9), is 0.087 and 0.060, for a and b, respectively).

4. Conclusions

Different types of adducts CF_3I- - -D (D = $(CH_3)_3N$, $(CH_3)_3P$, $(CH_3)_2S$ $(CH_3)_3NO$, $(CH_3)_3PO$, and DMSO) have been investigated. On the basis of our DFT calculations the CF_3I- - -ON-$(CH_3)_3$ adduct shows the strongest interaction energy (−7.81 kcal/mol, BBSE corrected) and the bonding energy trend is essentially determined by the orbital interaction term ΔE_{oi}.

TD-DFT calculations suggest that dispersion effects at the computed equilibrium distance of the adducts give only a small contribution to the total bonding energy.

All the studied adducts show a bonding energy comparable to that of the hydrogen bond (i.e., >2 kcal/mol), except the adduct **6′** (−0.94 kcal/mol, BSSE corrected), in which the I atom interacts with the S atom of the DMSO, for the steric term $\Delta E°$. All interaction energies have been calculated on geometries optimized at the (s.r.) ZORA level. Indeed, relativistic effects turn out to be very important for the correct description of I- - -X distance and interaction energy trends.

Acknowledgment. We thank Prof. Giuseppe Resnati for comments on a draft of the manuscript. Financial support through grants within COFIN 99 from the Italian Murst (Ministero dell'Università e della Ricerca Scientifica e Tecnologica) and computational resources from European Union and Regione Basilicata by the way of LaMI is gratefully acknowledged. P.R. thanks COFIN 99 for a fellowship.

TABLE 9: Mulliken Gross Population of Kohn−Sham SCF Orbitals of CF_3I and Donor D (D = $(CH_3)_3NO$, $(CH_3)_3PO$, DMSO) Fragments in 4, 5, 6′, 6″, and 6‴ Calculated at the s.r. ZORA Level

Γ			$4(^1A')^a$	$6''(^1A')^a$	$6'''(^1A')^a$	Γ			$5(^1A)^a$	$6'(^1A)^a$
A′	CF_3I	10a′	1.98	1.99	2.00	A	CF_3I	16a	1.99	2.00
		11a′ (LUMO)	0.14	0.08	0.05			17a (LUMO)	0.06	0.08
	D	10/8a′ (HOMO)[b]	1.88	1.93	1.97		D	16/13a (HOMO)[c]	1.96	1.93
A″	CF_3I	6a″ (LUMO)	1.99	2.00	2.00					
	D	6/5a″(HOMO)[b]	2.00	2.00	2.00					

[a] The ground-state configuration has been reported in parentheses. [b] 10a′ and 6a″ refer to HOMOs, in the A′ and A″ irreducible representations, respectively, of the adduct **4**, whereas 8a′ and 5a″ refer to the adducts **6″** and **6‴**. [c] 16a and 13a refer to HOMOs of the adducts **5** and **6′**, respectively.

References and Notes

(1) Reddy, D. S.; Craing, D. C.; Rae, A. D.; Desiraju, G. R. *J. Chem. Soc., Chem. Commun.* **1993**, 1737.

(2) Walsh, R. B.; Padgett, C. W.; Metrangolo, P.; Resnati, G.; Hanks, T. W., Pennington, W. T. *Cryst. Growth Des.* **2001**, *1*, 165.

(3) Bailey, R. D.; Grabarczyk, M.; Hanks, T. W.; Pennington, W. T. *J. Chem. Soc., Perkin Trans 2* **1997**, 2781. Cardillo, P.; Corradi, E.; Lunghi, A.; Meille, S. V.; Messina, M. T.; Metrangolo, P.; Resnati, G. *Tetrahedron* **2000**, *56*, 5535.

(4) Cardillo, P.; Corradi, E.; Lunghi, A.; Meille, S. V.; Messina, M. T.; Metrangolo, P.; Resnati, G. *Tetrahedron* **2000**, *56*, 5535.

(5) Amico, V.; Meille, S. V.; Corradi, E.; Messina, M. T.; Resnati, G. *J. Am. Chem. Soc.* **1998**, *120*, 8261.

(6) Corradi, E.; Meille, S. V.; Messina, M. T.; Metrangolo, P.; Resnati, G. *Tetrahedron Lett.* **1999**, *40*, 7519.

(7) Valerio, G.; Raos, G.; Meille, S. V.; Metrangolo, P.; Resnati, G. *J. Phys. Chem. A* **2000**, *104*, 1617.

(8) Antony, A.; Desiraju, G. R.; Jetti, R. K. R.; Kuduva, S. S.; Madhavi, N. N. L.; Nangia, A.; Thaimattam, R.; Thalladi, V. R. *Cryst. Eng.* **1998**, *1*, 1.

(9) Lommerse, J. P. M.; Taylor, R.; Allen, F. H. *J. Am. Chem. Soc.* **1996**, *118*, 3108.

(10) Grabowski, S. J. *J. Phys. Chem. A* **2001**, *105*, 10739.

(11) Fonseca Guerra, C.; Visser, O.; Snijders, J. G.; te Velde, G.; Baerends, E. J. Parallelisation of the Amsterdam Density Functional Program. In *Methods and Techniques of Computational Chemistry*; Clementi, E., Corongiu, G., Eds.; STEF: Cagliari, 1995.

(12) Pyykkö, P. *Chem. Rev.* **1988**, *88*, 563.

(13) van Lenthe, E. ZORA. Ph.D. Thesis, 1996, available on line at http://www.scm.com/Doc/publist.html.

(14) ADF STO basis set database available on line at http://tc.chem.vu.nl/SCM/DOC/atomicdata/.

(15) Becke, A. *Phy. Rev. A* **1988**, *38*, 3098.

(16) Perdew, J. P. *Phys. Rev. B* **1986**, *33*, 8822.

(17) Frisch, M. J.; Trucks, G. W.; Schlegel, H. B.; Scuseria, G. E.; Robb, M. A.; Cheeseman, J. R.; Zakrzewski, V. G.; Montgomery, J. A., Jr.; Stratmann, R. E.; Burant, J. C.; Dapprich, S.; Millam, J. M.; Daniels, A. D.; Kudin, K. N.; Strain, M. C.; Farkas, O.; Tomasi, J.; Barone, V.; Cossi, M.; Cammi, R.; Mennucci, B.; Pomelli, C.; Adamo, C.; Clifford, S.; Ochterski, J.; Petersson, G. A.; Ayala, P. Y.; Cui, Q.; Morokuma, K.; Malick, D. K.; Rabuck, A. D.; Raghavachari, K.; Foresman, J. B.; Cioslowski, J.; Ortiz, J. V.; Stefanov, B. B.; Liu, G.; Liashenko, A.; Piskorz, P.; Komaromi, I.; Gomperts, R.; Martin, R. L.; Fox, D. J.; Keith, T.; Al-Laham, M. A.; Peng, C. Y.; Nanayakkara, A.; Gonzalez, C.; Challacombe, M.; Gill, P. M. W.; Johnson, B. G.; Chen, W.; Wong, M. W.; Andres, J. L.; Head-Gordon, M.; Replogle, E. S.; Pople, J. A. *Gaussian 98*, revision A.7; Gaussian, Inc.: Pittsburgh, PA, 1998. (http://www.Gaussian.com/).

(18) (a) Binkley, J. S.; Pople, J. A.; Hehre, W. J. *J. Am. Chem. Soc.* **1980**, *102*, 939. (b) Gordon, M. S.; Binkley, J. S.; Pople, J. A.; Pietro, W. J.; Hehre, W. J. *J. Am. Chem. Soc.* **1982**, *104*, 2797. (c) Pietro, W. J.; Francl, M. M.; Hehre, W. J.; Defrees, D. J.; Pople, J. A.; Binkley, J. S. *J. Am. Chem. Soc.* **1982**, *104*, 5039. (c) Dobbs, K. D.; Hehre, W. J. *J. Comput. Chem*. **1986**, *7*, 359. (d) Dobbs, K. D.; Hehre, W. J. *J. Comput. Chem.* **1987**, *8*, 861. (e) Dobbs, K. D.; Hehre, W. J. *J. Comput. Chem.* **1987**, *8*, 880.

(19) Schafer, A.; Huber, C.; Ahlrichs, R. *J. Chem. Phys.* **1994**, *100*, 5829.

(20) (a) Hay, P. J.; Wadt, W. R. *J. Chem. Phys.* **1985**, *82*, 270. (b) Wadt, W. R.; Hay, P. J. *J. Chem. Phys.* **1985**, *82*, 284. (c) Hay, P. J.; Wadt, W. R. *J. Chem. Phys.* **1985**, *82*, 299.

(21) (a) Fuentealba, P.; Preuss, H.; Stoll, H.; Szentpaly, L. v. *Chem. Phys. Lett.* **1982**, *89*, 418. (b) Bergner, A., Dolg, M.; Kuechle, W.; Stoll, H.; Preuss, H. *Mol. Phys.* **1993**, *80*, 1431. (c) Fuentealba, P.; Szentpaly, L. v.; Preuss, H.; Stoll, H. *J. Phys. B* **1985**, *18*, 1287. (d) Igel-Mann, G.; Stoll, H.; Preuss, H. *Mol. Phys.* **1988**, *65*, 1321. (e) Kuechle, W.; Dolg, M.; Stoll, H.; Preuss, H. *Mol. Phys.* **1991**, *74*, 1245.

(22) (a) Ditchfield, R.; Hehre, W. J.; Pople, J. A. *J. Chem. Phys.* **1971**, *54*, 724. (b) Hehre, W. J.; Ditchfield, R.; Pople, J. A. *J. Chem. Phys.* **1972**, *56*, 2257. (c) Hariharan, P. C.; Pople, J. A. *Mol. Phys.* **1974**, *27*, 209. (d) Gordon, M. S. *Chem. Phys. Lett.* **1980**, *76*, 163. (e) Hariharan, P. C.; Pople, J. A. *Theor. Chim. Acta* **1973**, *28*, 213.

(23) Glukhovtsev, M. N.; Pross, A.; McGrath, M. P.; Radom, L. *J. Chem. Phys.* **1995**, *103*, 1878.

(24) Becke, A. D. *J. Chem. Phys.* **1993**, *98*, 5648.

(25) Ziegler, T.; Rauk, A. *Theor. Chim. Acta* **1977**, *46*, 1.

(26) Ziegler, T.; Rauk, A. *Inorg. Chem.* **1979**, *18*, 1558.

(27) Ziegler, T. In *Metal−Ligand Interations: From Atoms, to Clusters, to Surfaces*; Salahub, D. R., Russo, N., Eds.; NATO ASI Series Vol. 378; Kluwer Academic Publishers: Dordrecht, The Netherlands, 1992; p 367.

(28) van Leeuwen, R.; Baerends, E. J. *Phys. Rev. A* **1994**, *49*, 2421.

(29) Van Gisbergen, S. J. A. Molecular response property calculations using time-dependent density functional theory. Ph.D. Thesis, 1998, available on line http://www.scm.com/Doc/publist.html.

(30) Osinga, V. P.; Van Gisbergen, S. J. A.; Snijders, J. G.; Baerends, E. J. *J. Chem. Phys.* **1997**, *106*, 5091.

(31) Boys, S. F.; Bernardi, F. *Mol. Phys.* **1970**, *19*, 553.

(32) Messina, M. T.; Metrangolo, P.; Panzeri, W., Pilati, T., Resnati, G. *Tetrahedron* **2001**, *57*, 8543.